The Onset of Ion Heating During Magnetic Reconnection with a Strong Guide Field

J. F. Drake[1, a)] and M. Swisdak[2, b)]
[1)] *University of California, Berkeley, CA 94720*
[2)] *University of Maryland, College Park, MD 20742*

(Dated: 1 May 2014)

The onset of the acceleration of ions during magnetic reconnection is explored via particle-in-cell simulations in the limit of a strong ambient guide field that self-consistently and simultaneously follow the motions of protons and α particles. Heating parallel to the local magnetic field during reconnection with a guide field is strongly reduced compared with the reconnection of anti-parallel magnetic fields. The dominant heating of thermal ions during guide field reconnection results from pickup behavior of ions during their entry into reconnection exhausts and dominantly produces heating perpendicular rather than parallel to the local magnetic field. Pickup behavior requires that the ion transit time across the exhaust boundary (with a transverse scale of the order of the ion sound Larmor radius) be short compared with the ion cyclotron period. This translates into a threshold in the strength of reconnecting magnetic field that favors the heating of ions with high mass-to-charge. A simulation with a broad initial current layer produces a reconnecting system in which the amplitude of the reconnecting magnetic field just upstream of the dissipation region increases with time as reconnection proceeds. The sharp onset of perpendicular heating when the pickup threshold is crossed is documented. A comparison of the time variation of the parallel and perpendicular ion heating with that predicted based on the strength of the reconnecting field establishes the scaling of ion heating with ambient parameters both below and above the pickup threshold. The relevance to observations of ion heating in the solar corona is discussed.

arXiv:1404.7795v1 [physics.plasm-ph] 30 Apr 2014

I. INTRODUCTION

The production of energetic particles during flares remains a central unsolved issue in solar physics. Extensive observational evidence indicates that a substantial fraction of the energy released during a flare rapidly accelerates charged particles, with electrons reaching $\mathcal{O}(1)$ MeV and ions $\mathcal{O}(1)$ GeV/nucleon[1]. Explaining such energy gain requires accounting not only for the relevant energy and time scales but also the resulting spectra, which exhibit a common shape for most ion species. At the same time, high mass-to-charge ions are greatly overrepresented in flares, with abundances as much as two orders of magnitude higher than normal coronal values[2,3].

Magnetic reconnection is the ultimate energy source in impulsive flares. Thus, in many theories reconnection plays a direct role in particle acceleration through DC electric fields[4], interactions with multiple magnetic islands[5] or first-order Fermi acceleration in contracting and merging islands[6–9]. On the other hand, in some models reconnection serves as a source of magnetohydrodynamic (MHD) waves[10,11] or shocks[12,13] that then independently drive particle acceleration.

The release of magnetic energy during reconnection dominantly takes place downstream of the x-line in the exhaust where newly reconnected field lines expand to relax their magnetic tension and drive Alfvénic outflows. The characteristic outflow speed is given by $c_{Axup} = B_{xup}/\sqrt{4\pi m_p n_{up}}$, with B_{xup} and n_{up} the reconnecting component of the magnetic field and density just upstream of the exhaust. In the MHD description the dominant heating during reconnection of anti-parallel magnetic fields is produced by the switch-off Petschek shocks that bound the exhaust[14]. These shocks also drive the Alfvénic outflow. In the kinetic description, ions moving across the exhaust are slung by the fast moving field lines. The resulting counterstreaming ion distributions produce a large effective parallel temperature $T_\parallel \sim m_i c_{Ax}^2$ with minimal perpendicular heating[15,16]. The associated pressure anisotropy prevents the formation of the Petschek switch-off shock[17,18].

Coronal reconnection, however, typically involves a substantial guide field (the magnetic field component perpendicular to the plane of reconnection). In reconnection with a guide field the MHD model produces a pair of rotational discontinuities (RDs) that bound the exhaust and produce the magnetic field rotation that drives the outflow. A pair of parallel shocks within the exhaust compress and heat the ions. An important question is whether the MHD description is valid in the typical coronal environment where the particle scattering mean-free-path is relatively long. In a kinetic description the RDs that bound the exhaust collapse to the scale of the proton sound Larmor radius $\rho_s = c_s/\Omega_p$, where $c_s = \sqrt{(T_e + T_p)/m_p}$ is the sound speed and Ω_p is the proton cyclotron frequency[19]. If the crossing time of ions (of any species) through the RD is longer than their cyclotron time, the ions will cross the RD with little heating and will counterstream across the exhaust to produce an

[a)] drake@umd.edu; permanent address: University of Maryland, College Park, MD 20742
[b)] swisdak@umd.edu

increment in the effective parallel temperature[19],

$$\Delta T_{\parallel} = m_i c_{Axup}^2 B_{xup}^2 / B_{up}^2, \quad (1)$$

with $\Delta T_{\perp} \sim 0$. The ambient guide field reduces the parallel heating compared with the case of anti-parallel reconnection. If the crossing time of ions through the RD is shorter than their cyclotron time, the ions entering into the exhaust are not able to follow the rapid change in the direction of the magnetic field and become non-adiabatic. They effectively behave like pickup particles since they are initially at rest in the Alfvénic flow of the exhaust[19,20]. As they are "picked up" by the exhaust they gain an effective thermal velocity c_{Axup}. Because of the strong guide field the temperature increment is perpendicular to the local magnetic field ($\Delta T_{\parallel} \sim 0$) and is given by

$$\Delta T_{\perp} = m_i c_{Axup}^2 / 2, \quad (2)$$

with m_i the mass of the relevant ion species – heavier ions gain more energy. Note that for $B_{zup}^2 \gg B_{xup}^2$ the heating in the pickup regime greatly exceeds that in the non-pickup regime. The criterion for pickup behavior translates into

$$\frac{m_i}{Z_i m_p} > \left(\frac{1}{r\pi\sqrt{2}}\right)\sqrt{\beta_{xup}}, \quad (3)$$

where $r = v_{in}/c_{Axup} \sim 0.1$ is the normalized rate of reconnection, $\beta_{xup} = 8\pi n_{up}(T_e + T_p)/B_{xup}^2$ is the ratio of plasma to magnetic pressure based on the reconnection magnetic field just upstream of the exhaust and Z_i is the ion charge state. High mass-to-charge ions satisfy this criterion more easily than protons.

Classical collisions are often not negligible in the corona so an important question is whether classical resistive diffusion of the magnetic field is sufficient to broaden the RD beyond the Larmor scale ρ_s. Balancing convection of magnetic flux through the RD with resistive diffusion $\eta c^2/4\pi$ yields an equation for the limiting width Δ,

$$\frac{v_{in}}{\Delta} \sim \frac{\eta c^2}{4\pi\Delta^2} \quad (4)$$

or

$$\Delta \sim \frac{\eta c^2}{4\pi r c_{Ax}}. \quad (5)$$

For typical solar parameters ($T \sim 100eV$, $n \sim 10^9 cm^{-3}$, $B \sim 50G$) with $r \sim 0.1$ we find $\Delta \sim 10^{-4} cm$, much shorter than $\rho_s \sim 30cm$. Thus, classical collisions are insufficient to broaden the RD beyond ρ_s and are therefore unimportant. The collisionless model of the RD should correctly describe the dynamics.

The solar corona is normally considered a low β medium and therefore one might expect the inequality in Eq. (3) for pickup behavior to be easily satisfied. However, prior to the onset of reconnection ambient current layers are likely to be macroscopic and for this reason when reconnection first onsets the magnetic field just upstream of the reconnection region B_x will be very small. B_x will then increase in time as the larger magnetic field upstream convects toward the reconnection site. Thus, at the start of reconnection all ions will be in the adiabatic regime because β_x will be large and energy going into ion heating compared with that associated with the bulk flow will be small. As β_x drops as reconnection proceeds each ion species will sequentially (based on their mass-to-charge) move into the pickup regime. Once protons have entered the pickup regime the fraction of released magnetic energy going into ion heat will be comparable to that in the bulk flow.

Consistent with this picture, observations have revealed that in the extended solar corona, $T_{\perp} \gg T_{\parallel}$[21,22], suggesting that magnetic reconnection is a potential heating mechanism for the large-scale corona. Earlier there was an assumption that the observations of $T_{\perp} \gg T_{\parallel}$ in the corona argued in favor of ion heating by ion cyclotron waves[23]. This assumption needs to be re-examined. Further, if the pickup scenario for ion heating during reconnection is correct, the lower threshold for strong ion heating for high mass-to-charge ions might be a mechanism for the abundance enhancement of such ions in impulsive flares[3] as an alternative to proposed wave mechanisms[11,24,25].

In this manuscript we explore the onset of pickup behavior and associated strong ion heating during reconnection using a particle-in-cell (PIC) code with an initial state with a wide current layer and a strong ambient guide field. We include two ion species, protons and α particles, so that we can separate the onset of ion heating based on mass-to-charge. Early in the simulation the heating of both species is weak. As reconnection develops, the upstream value of β_x decreases and the αs undergo a sharp transition to strong perpendicular heating. The threshold for this transition is close to that given in Eq. (3). The protons in contrast remain below the threshold for pickup behavior and do not exhibit the onset of strong perpendicular heating. Because the exhaust velocity of the simulation varies over a substantial range (as B_x increases monotonically), the scaling of parallel and perpendicular heating with the exhaust outflow velocity is obtained and compared with the predictions in Eqs. (1) and (2). The simulations therefore establish the fundamental properties of ion heating during reconnection with a guide field and lay the groundwork for understanding ion heating in the extended corona and during impulsive flares and in other astrophysical and laboratory systems.

II. NUMERICAL SIMULATIONS

We carry out simulations using the code `p3d`[26]. Like all PIC codes, it tracks individual particles ($\approx 10^9$ in this work) as they move through electromagnetic fields

defined on a mesh. Unlike more traditional fluid representations (e.g., MHD), PIC codes correctly treat small lengthscales and fast timescales, which are particularly important for understanding the x-line and separatrices during magnetic reconnection.

The simulated system is periodic in the $x-y$ plane, where flow into and away from the x-line are parallel to $\hat{\mathbf{y}}$ and $\hat{\mathbf{x}}$, respectively, and the guide magnetic field and reconnection electric field are parallel to $\hat{\mathbf{z}}$. The initial magnetic field and density profiles are based on the Harris equilibrium. The reconnecting magnetic field is given by $B_x = \tanh[(y-L_y/4)/w_0] - \tanh[(y-3L_y/4)/w_0] - 1$, where w_0 and L_y are the half-width of the current sheets and the box size in the $\hat{\mathbf{y}}$ direction. Particles are distributed in a constant-density background and two current sheets in which the density rises in order to maintain pressure balance with the magnetic field. We initiate reconnection with a small perturbation that produces a single magnetic island on each current layer.

The code is written in normalized units in which magnetic fields are scaled to the asymptotic value of the reversed field B_{0x}, densities to the value at the center of the initial current sheets minus the uniform background density, velocities to the proton Alfvén speed $c_A = B_{0x}/\sqrt{4\pi m_p n_0}$, times to the inverse proton cyclotron frequency in B_{0x}, $\Omega_{p0x}^{-1} = m_p c/eB_{0x}$, lengths to the proton inertial length $d_p = c_A/\Omega_{p0x}$ and temperatures to $m_p c_A^2$.

The proton-to-electron mass ratio is taken to be 25 in order to minimize the difference between pertinent length scales and hence simulate as large a domain as possible. It has been shown[27–29] that the rate of reconnection and structure of the outflow exhaust do not depend on this ratio. Since the ion heating examined here depends only on the exhaust geometry, we also expect our results to be insensitive to the mass ratio. The simulation assumes $\partial/\partial z = 0$, i.e. that field and particle quantities do not vary in the out-of-plane direction, making this a two-dimensional simulation.

In addition to protons and electrons, we also include a number density of 4% $^4\mathrm{He}^{++}$ (α) particles in the background particle population with an initial temperature equal to that of the electrons and protons. This number density does not affect the reconnection dynamics appreciably, while still providing a large sample of particles with $m_i/m_p Z_i > 1$ that can be used to test the scaling of the onset relation for pickup behavior given in Eq. (3).

In Fig. 1 we show an overview of results from a simulation with a computational domain $L_x \times L_y = 102.4 \times 51.2\, d_p$ and an initial guide field $B_{0z} = 2.0 B_{0x}$ at $t = 600\Omega_{p0x}^{-1}$. The grid spacing for this run is $0.025\, d_p$, the electron, proton, and α temperatures, $T_e = T_p = T_\alpha = 0.25 m_p c_A^2$, are initially uniform, and the velocity of light is $15 c_A$. The half-width of the initial current sheet, w_0, is $7\, d_p$ and the background density is $0.2 n_0$. Panel (a) depicts the total out-of-plane current density J_z centered around the x-line of one of the current sheets.

Ambient plasma from above and below slowly flow toward the current sheet while embedded in oppositely directed magnetic fields (pointing to the right above the layer and to the left below). Reconnected field lines are bent and, to reduce their magnetic tension, rapidly move away from the x-line, dragging plasma with them. In Fig. 1(b) is the proton outflow velocity v_{px}. In Fig. 1(c) is E_y, which is the electric field that spans the exhaust during reconnection with a guide field and forces $\mathbf{E}\cdot\mathbf{B} \sim E_y B_y + E_z B_z \sim 0$. Thus, $E_y \sim E_z B_z/B_y$[19] and since $B_y \sim 0.1 B_x \ll B_z$, E_y is much greater than the reconnection electric field E_z. E_y controls the outflow with $v_{px} \sim cE_y/B_z$, which is the reason for the similarity between v_{px} and E_y in Fig. 1. Because E_y is the dominant component of $\mathbf{E}$, it is also the driver of ion heating during the pickup process[19].

The data shown in Fig. 1 is at late time after the reconnecting magnetic field B_x just upstream of the x-line is large. The time development of B_x and the density n in cuts across the x-line (through $x = 77 d_p$ in Fig. 1) are shown in Fig. 2 at $t = 0$, $t = 450\Omega_{pi}^{-1}$,$t = 560\Omega_{pi}^{-1}$ and $t = 600\Omega_{pi}^{-1}$. The current layer is initially broad with a high density in the center of the sheet. As time passes, the magnetic field convects inward toward the x-line at $y = 0$. The magnetic field upstream of the current layer therefore increases with time. At the same time lower density plasma also convects toward the x-line (the asymmetry in the cut in the density is a consequence of the density cavities that develop during reconnection with a guide field[30]). The consequence is that the increasing magnetic field and lower density causes the Alfvén speed c_{Axup} based on the parameters just upstream of the strong current layer at the x-line to increase dramatically. The exhaust velocity therefore also increases with time. The relationship between the peak outflow velocity v_{px} and c_{Axup} is shown in Fig. 3. The individual data points correspond to different times as reconnection develops. At late time v_{px} is very close to c_{Axup}, as expected from the Walén relation[31].

III. ION PICKUP AND HEATING

Particle acceleration is controlled by the structure and magnitude of the electric field, which, for such a strong guide field, is dominated by E_y. Particles enter the exhaust with velocity $v_y \sim 0.1 c_{Ax}$. The non-adiabatic particles cross the boundary in a time that is short compared with their cyclotron period and are essentially at rest in the simulation frame while the outflow streams past at roughly the Alfvén speed. The trajectories of non-adiabatic particles are cycloids which can be represented by an $\mathbf{E}\times\mathbf{B}$ drift plus an effective "thermal velocity" equal to the Alfvén speed. The dynamics is analogous to that of stationary neutral atoms surrounded by the moving solar wind. When they are ionized, the new ion first moves in the direction of the motional electric field in order to gain the necessary energy to flow with the rest of the wind. As it gets "picked up", it gains a thermal

velocity equal to the solar wind velocity[32].

In Fig. 1 we show the temperatures of both species parallel and perpendicular to the local magnetic field at $t = 600\Omega_{ci}^{-1}$. In (d) and (e) are the perpendicular and parallel temperatures of the protons while in (f) and (g) are the corresponding temperatures of the α particles. The α temperature increase in the direction perpendicular to $\mathbf{B}$ is much greater than its parallel temperature and also much greater than that of the protons (note the different scales of the color bars). The α heating is more than mass-proportional, which would be the expected value if both species had the same thermal speed.

In Fig. 4 we show the time-development of the proton and alpha temperature increment as well as the evolution of the upstream value of β_{xup}. In Fig. 4(a) are the increments of the perpendicular temperatures of the αs (solid) and protons (dashed). There is a sharp increase in the rate of increase of the α perpendicular temperature at $t = 563\Omega_{p0x}^{-1}$. This corresponds to $\beta_{xup} \sim 1$ (Fig. 4(c)), which is at a somewhat higher value than the predicted onset at $\beta_{xup} \sim 0.79$ given in Eq. (3. By contrast the protons exhibit no sharp onset of perpendicular heating. Their perpendicular heating onset should occur at $\beta_{xup} \sim 0.2$, which is not reached by the end of the simulation. A simulation carried out with a lower initial upstream temperature would enable us to document the pickup onset of the protons. In Fig. 4(b) are the parallel temperature increments of the αs (solid) and the protons (dashed). The α parallel heating is well below the perpendicular heating but is larger than expected at late time when the αs are in the pickup regime and the increment of the parallel temperature should be very small. This might be due to scattering. The spatial location of the α perpendicular and parallel heating overlap (Figs. 1(f) and (g)) while the peaks in the proton parallel and perpendicular heating in Figs. 1 do not. The proton parallel temperature increment is modestly greater than that in the perpendicular temperature, which is consistent with the protons remaining adiabatic.

The ion perpendicular temperature increment is plotted versus the expected value in the pickup regime for the protons (Fig. 3(b)) and the αs (Fig. 3(c)). The proton temperature increment is far below that which would be expected in the pickup regime (by nearly an order of magnitude). This is consistent with the protons being adiabatic through the end of the simulation. The αs by contrast have temperature increments within a factor of two of the expected value for the larger values of c_{Axup} when the αs are in the pickup regime. The slope of the line in Fig. 3(c) is 0.54 while that expected from Eq. (2) is 1.0. Further, that a straight line fits through the high c_{Axup} data indicatesg that $\Delta T_{\perp\alpha} \propto c_{Axup}^2$ as expected. For the lower values of c_{Axup}, when the αs are adiabatic, $\Delta T_{\perp\alpha}$ is well below that predicted in the pickup regime and does not scale as c_{Axup}^2. One reason that the α perpendicular heating in the pickup regime from this simulation is somewhat less than expected is because of a time delay in the α heating relative to v_{px} associated with the time required for the αs to be picked up by the exhaust. This is not physically significant but is a consequence of the fact that in the simulation at late time v_{px} and $T_{\perp\alpha}$ are both rapidly increasing (Fig. 4).

Finally, in Fig. 5 we show $T_\parallel$ versus the predicted value in Eq. (1) (the adiabatic regime) for protons and αs. In the adiabatic regime the perpendicular heating is small and the ion heating falls well below the usual scaling $\Delta T_\parallel \sim m_i c_{Ax}^2$ in the absence of a guide field. The measured value of $\Delta T_{\parallel p}$ scales as expected but is smaller by about a factor of two (the slope of the line in Fig. 5 is 0.54 compared with the expected value of 1.0 in Eq. (1)). The data falls significantly below the straight line at high values of B_{xup}, which corresponds to data when the protons are approaching the adiabatic regime and $\Delta T_{\parallel p}$ is expected to drop. The parallel heating of αs, while scaling as expected, is well below the expected value (the slope of the line in Fig. 5 is 0.15 compared with a slope of 1.0 in Eq. (1)). The reason for the shortfall is not known.

IV. DISCUSSION

Magnetic reconnection in the corona and many laboratory experiments typically involves a large guide field. In this regime we have shown that ion heating at the Rotational Discontinuities (RDs) that form at the boundaries of outflow exhausts greatly exceeds that expected from the slow shocks of the MHD model when ions are in the pickup regime (see Eq. (3)). For typical coronal parameters of $B = 50$G and $n = 10^9/\text{cm}^3$, energy increments of ≈ 25 keV/nucleon are expected. The temperature increment is dominantly perpendicular to the local magnetic field and the released magnetic energy going into heating ions in this regime is comparable to that associated with the bulk flow. Ions in the adiabatic regime are only weakly heated, heating is parallel to the magnetic field and in this regime the energy going into heating ions is much smaller than the energy going into bulk flow.

Observations have revealed that the abundances of high mass-to-charge ions ions are enhanced in solar flares, with the strength of the enhancement depending only on M/Q. The fact that non-adiabatic behavior and the associated strong heating depends on M/Q suggests that reconnection might be able to explain the abundance enhancements in impulsive flares. Furthermore, the increase in $T_\perp/T_\parallel$ in the exhaust seen here is consistent with that observed in the extended corona[21,22]. Strong perpendicular heating of high mass-to-charge ions is also seen in laboratory Reversed Field Pinch experiments during global sawtooth events[33,34].

The kinetic energy of ions picked up during reconnection in the solar corona of ≈ 25 keV/nucleon, although significantly above thermal energies, falls short of the inferred maximal energies of ≈ 1 GeV. Further acceleration can occur via interactions with the multiple magnetic islands predicted to be produced during flares[6]. Super-

Alfvénic ions trapped within a slowly contracting island can repeatedly reflect from the ends, gaining energy via a first-order Fermi process, and producing power-law spectra consistent with observations[7,35]. Thermal ions cannot be accelerated by this process because their bounce time is greater than the timescale for island contraction. Thus, the pickup process can act as a seed mechanism for further energy gain and may ultimately control the abundances of ions measured in impulsive flares. A realistic test of this scenario requires 3-D simulations of multiple x-lines and multiple islands, something which is not currently computationally feasible. Simulations of multiple current layers in a 2-D model, however, will enable us to explore both the pickup process and subsequent heating through island merging and contraction.

Observations of reconnection at the magnetopause as, for example, carried out for electrons[36] should yield data for $T_\parallel$ and $T_\perp$ for both protons and α particles in order to test the mechanism discussed here. Provided the instrumentation can differentiate between different M/Q ions, data collected by the upcoming Solar Probe Plus mission, with a planned perihelion of $\approx 9R_\odot$ (which lies within the outer corona), should also be able put our predictions to the test.

Finally, it is widely believed that some process converts a fraction of the energy found in the convective motions of the solar photosphere into the heat that ensures the continuous existence of a $\mathcal{O}(10^6$ K) corona and accelerates the solar wind. Broadly speaking, the two most likely candidates are wave heating — in which oscillations generated in the photosphere travel into the corona, develop into turbulence, and dissipate — and reconnection, in which the topological reorganization of the magnetic field releases energy and heats the plasma. Measurements by the Solar Ultraviolet Measurements of Emitted Radiation (SUMER) and Ultraviolet Coronal Spectrometer (UVCS) instruments of the SOHO (Solar and Heliospheric Observatory) spacecraft provide significant constraints on any theory of coronal heating. In particular, at heights of $2-3R_\odot$ protons have a slight temperature anisotropy with $T_\perp > T_\parallel$ while heavier ions (represented by O^{5+}) are strongly anisotropic, with $T_\perp/T_\parallel \gtrsim 10$[21,22]. Interestingly, the process discussed in this work should be active in the region in question and produces temperature anisotropies consistent with these results.

ACKNOWLEDGMENTS

This work has been supported by NSF Grant AGS1202330 and NASA grants APL-975268 and NNX08AV87G. Computations were carried out at the National Energy Research Scientific Computing Center.

[1] A. G. Emslie et al., J. Geophys. Res. **109**, A10104 (2004).
[2] G. M. Mason, J. E. Mazur, and D. C. Hamilton, Astrophys. J. **425**, 843 (1994).
[3] G. M. Mason, Space Sci. Rev. **130**, 231 (2007).
[4] G. D. Holman, ApJ **293**, 584 (1985).
[5] M. Onofri, H. Isliker, and L. Vlahos, Phys. Rev. Lett. **96**, 151102 (2006).
[6] J. F. Drake, M. Swisdak, K. M. Schoeffler, B. N. Rogers, and S. Kobayashi, Geophys. Res. Lett. **33**, 13105 (2006).
[7] J. F. Drake, M. Opher, M. Swisdak, and J. N. Chamoun, ApJ **709**, 963 (2010).
[8] M. Oka, T. D. Phan, S. Krucker, M. Fujimoto, and I. Shinohara, ApJ **714**, 915 (2010).
[9] G. Kowal, E. M. de Gouveia Dal Pino, and A. Lazarian, ApJ **735**, 102 (2011).
[10] J. A. Miller, Space Sci. Rev. **86**, 79 (1998).
[11] V. Petrosian and S. Liu, Astrophys. J. **610**, 550 (2004).
[12] D. C. Ellison and R. Ramaty, ApJ **298**, 400 (1985).
[13] B. V. Somov and R. Kosugi, ApJ **485**, 859 (1997).
[14] H. E. Petschek, Magnetic field annihilation, in *AAS/NASA Symposium on the Physics of Solar Flares*, edited by W. N. Ness, page 425, NASA, Washington, DC, 1964.
[15] M. Hoshino, T. Mukai, and T. Yamamoto, J. Geophys. Res. **103**, 4509 (1998).
[16] J. T. Gosling, R. M. Skoug, and D. J. McComas, Geophys. Res. Lett. **110**, A01107 (2005).
[17] Y.-H. Liu, J. F. Drake, and M. Swisdak, Phys. Plasmas **19**, 022110 (2012).
[18] K. Higashimori and M. Hoshino, J. Geophys. Res. **117**, 1220 (2012).
[19] J. F. Drake, P. A. Cassak, M. A. Shay, M. Swisdak, and E. Quataert, ApJ **700**, L16 (2009).
[20] K. Knizhnik, M. Swisdak, and J. F. Drake, ApJ Lett. **743**, L35 (2011).
[21] J. L. Kohl et al., Solar Phys. **175**, 613 (1997).
[22] J. L. Kohl et al., ApJ **501**, 127 (1998).
[23] S. R. Cranmer and A. A. van Ballegooijen, ApJ **594**, 573 (2003).
[24] J. A. Miller et al., J. Geophys. Res. **102**, 14631 (1997).
[25] S. Liu, V. Petrosian, and G. M. Mason, Astrophys. J. **636**, 462 (2006).
[26] A. Zeiler et al., J. Geophys. Res. **107**, 1230 (2002), doi:10.1029/2001JA000287.
[27] M. A. Shay and J. F. Drake, Geophys. Res. Lett. **25**, 3759 (1998).
[28] M. Hesse, K. Schindler, J. Birn, and M. Kuznetsova, Phys. Plasmas **5**, 1781 (1999).
[29] M. A. Shay, J. F. Drake, and M. Swisdak, Phys. Rev. Lett. **99**, 155002 (2007).
[30] P. L. Pritchett and F. V. Coroniti, J. Geophys. Res. **109**, A01220 (2004).
[31] B. U. Ö. Sonnerup et al., J. Geophys. Res. **86**, 10049 (1981).
[32] E. Mobius et al., Nature **318**, 426 (1985).
[33] S. Gangadhara et al., Phys. Rev. Lett. **98**, 075001 (2007).
[34] G. Fiksel et al., Physical Review Letters **103**, 145002 (2009).
[35] J. F. Drake, M. Swisdak, and R. Fermo, ApJ Lett. **763**, L5 (2013).
[36] T. D. Phan et al., Geophys. Res. Lett. **40**, 4475 (2013).

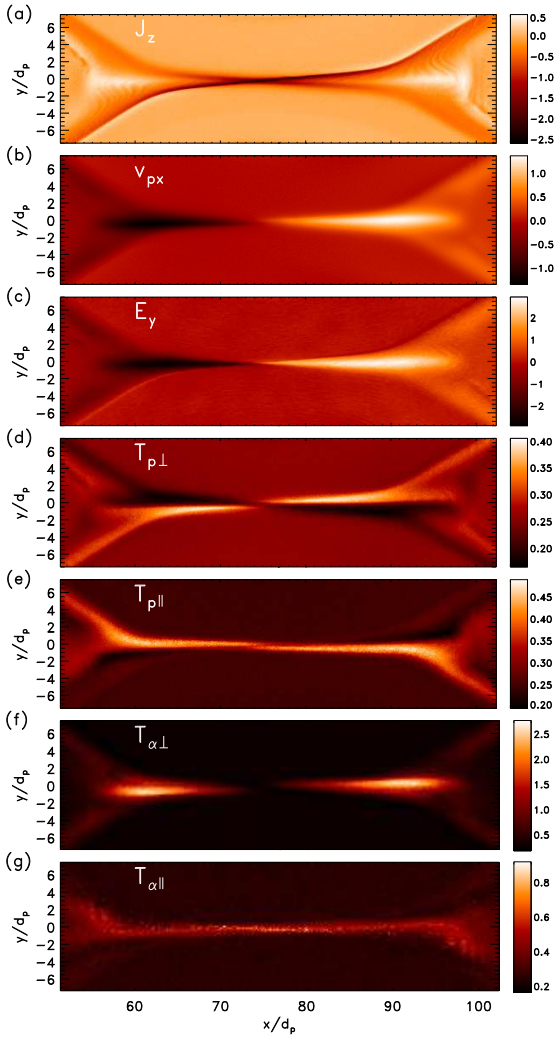

FIG. 1. (color online) Overview of a PIC simulation with an initial guide field $B_{0z} = 2B_{0x}$ at time $t = 600\Omega_{p0x}^{-1}$. In (a) the total out-of-plane current density J_z; in (b) the proton outflow velocity v_{px}; in (c) the transverse electric field E_y; in (d) the proton perpendicular temperature $T_{p\perp}$; in (e) the proton parallel temperature $T_{p\parallel}$; in (f) the α perpendicular temperature $T_{\alpha\perp}$; and in (g) the α parallel temperature $T_{\alpha\parallel}$

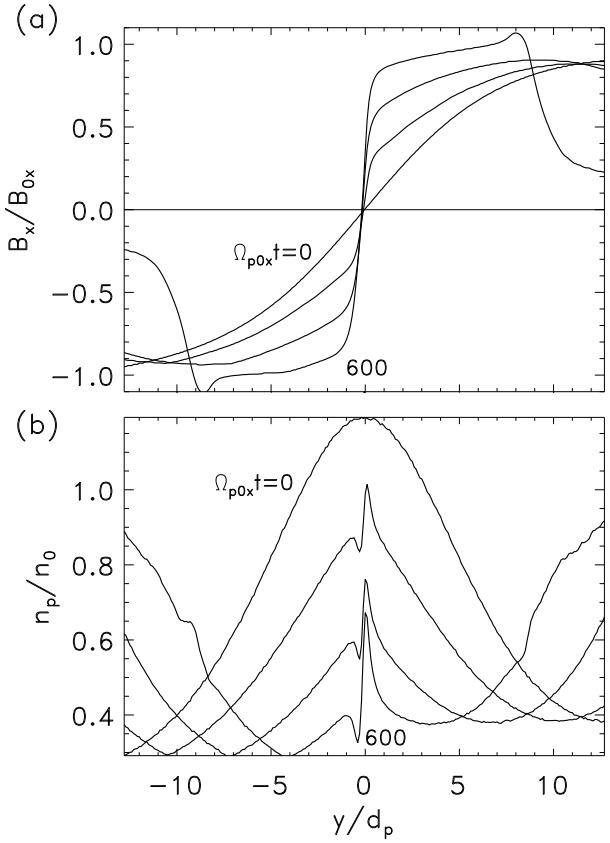

FIG. 2. Cuts across the current layer of the reconnection field B_x and the proton density n at $t = 0$, $t = 450\Omega_{p0x}^{-1}$,$t = 560\Omega_{p0x}^{-1}$ and $t = 600\Omega_{p0x}^{-1}$.

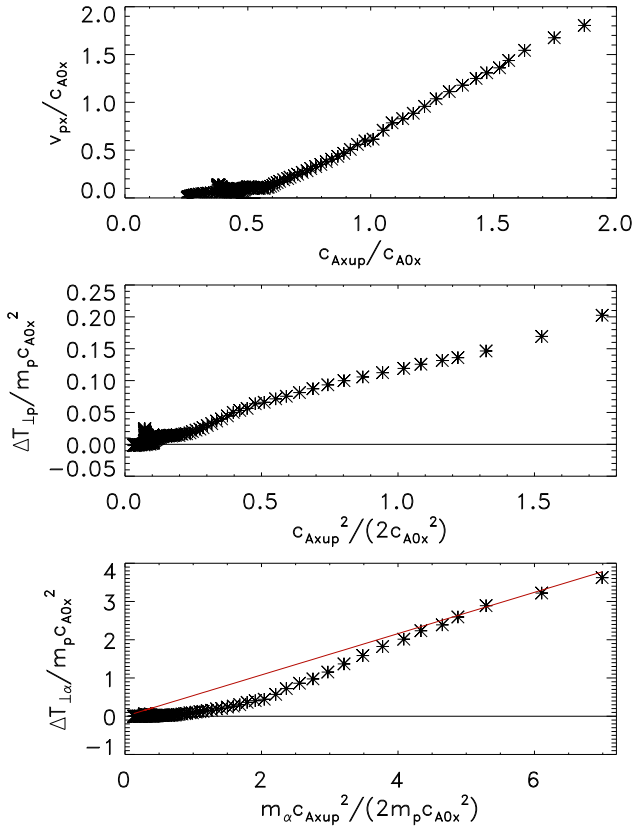

FIG. 3. (color online) The (a) peak proton exhaust velocity v_{px} and the increments in the peak (b) proton and (c) α perpendicular temperatures versus their expected values in the pickup regime (Eq. (2)). The solid line in (c) has a slope of 0.54

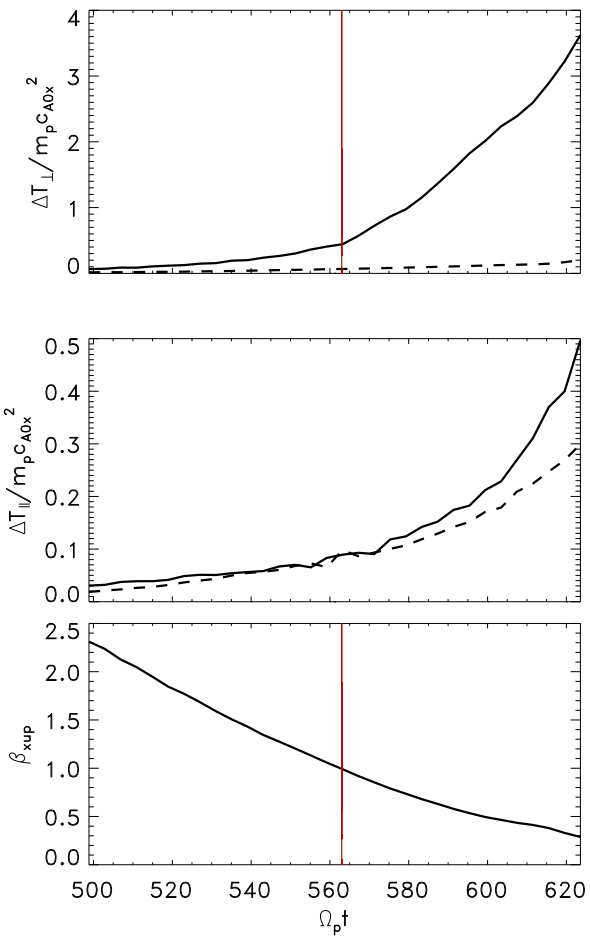

FIG. 4. (color online) The time dependence of the increments in the proton (dashed) and α (solid) (a) perpendicular and (b) parallel temperatures and (c) the upstream value of $\beta_x = 8\pi n(T_i + T_e)/B_x^2$. The vertical solid lines in (a) and (c) mark the onset of strong perpendicular heating of the αs.

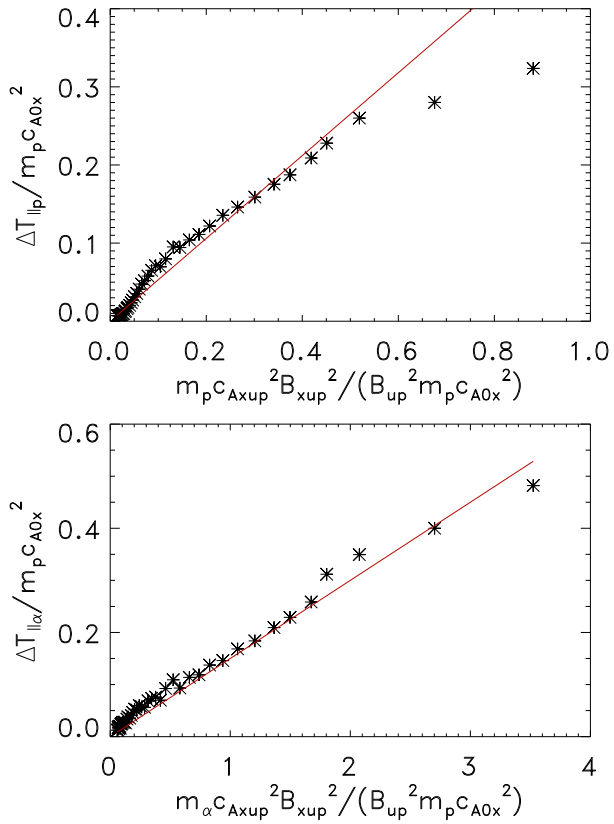

FIG. 5. (color online) The increments in the (a) proton and (b) α parallel temperatures versus their expected values in Eq. (1) in the adiabatic regime. The solid line in (a) has a slope of 0.53 and in (b) a slope of 0.15.